33rd Annual International Conference of the IEEE EMBS
Boston, Massachusetts USA, August 30 - September 3, 2011

Analysis of the Respiratory Flow Cycle Morphology in Chronic Heart Failure Patients Applying Principal Components Analysis

Ainara Garde, *Member, IEEE,* Beatriz F. Giraldo, *Member, IEEE,* Leif Sörnmo, *Senior Member, IEEE,* and Raimon Jané, *Member, IEEE*

***Abstract*— The study of flow cycle morphology provides new information about the breathing pattern. This study proposes the characterization of cycle morphology in chronic heart failure patients (CHF) patients, with periodic (PB) and non-periodic breathing (nPB) patterns, and healthy subjects. Principal component analysis is applied to extract a respiratory cycle model for each time segment defined by a 30-s moving window. To characterize morphology of the model waveform, a number of parameters are extracted whose significance is evaluated in terms of the following three classification problems: CHF patients with either PB or nPB, CHF patients versus healthy subjects, and nPB patients versus healthy subjects. 26 CHF patients (8 with PB and 18 with non-periodic breathing pattern (nPB)) and 35 healthy subjects are studied. The results show that a respiratory cycle compressed in time characterizes PB patients, i.e., shorter inspiratory and expiratory periods, and higher dispersion of the maximum inspiratory and expiratory flow value (accuracy of 87%). The maximal expiratory flow instant occurs earlier in CHF patients than in healthy subjects (accuracy of 87%), with a steeper slope between inspiration and expiration. It is also found that the standard deviation of the expiratory period, evaluated for each subject, is much lower in CHF patients than in healthy subjects. The maximal expiratory flow instant occurs earlier (accuracy of 84%) in nPB patients, when comparing subjects with similar respiratory pattern like nPB patients and healthy subjects.**

I. INTRODUCTION

Principal component analysis (PCA) is a very popular linear data transformation technique for feature extraction and data dimensionality reduction in statistical pattern recognition and signal processing. The principal components are derived as a linear combination of the variables of the data set, with weights chosen so that the principal components become mutually uncorrelated. Each component contains new information about the data set, and is ordered so that the first few components account for most of the variance [1], [2].

Principal component analysis is often employed for the study of waveform morphology in different biomedical signals. It permits a rather robust feature extraction of various waveform properties when tracking temporal changes of a signal. Castells et al. [3] present an overview of PCA in different ECG signal processing applications.

Chronic heart failure (CHF) is associated with major abnormalities of autonomic cardiovascular control, and is characterized by enhanced sympathetic nerve activity and cardiorespiratory disarrangement. CHF patients often develop breathing anomalies such as various forms of oscillatory breathing patterns characterized by rises and falls in ventilation. Several studies have shown that alternating cycles of hyper- and hypoventilation provoke oscillations in blood pressure, heart rate, and tidal volume, and that this leads to a state of physiological instability in the already stressed cardiovascular system [4]. Thus, abnormal breathing patterns can promote the progression of heart failure and cause increased mortality. Previous studies present periodic breathing (PB) during sleep or wakefulness as a powerful predictor of poor prognosis in CHF patients [5]. Various studies report a PB prevalence as high as 70% in these patients [6]. It is therefore crucial to establish accurate risk stratification of CHF patients so as to optimize the allocation of limited resources. The number of available treatment options have increased, but this increase has rendered clinical decision making far more complex.

In our previous studies we characterized the respiratory pattern in CHF patients through the envelope of the respiratory flow signal [7], and by applying the correntropy to the respiratory flow signal [8]. In this paper, we explore PCA for studying the morphology of respiratory flow cycles in CHF patients (both PB and nPB) and healthy subjects.

II. METHODS

A. Principal component analysis

When the signal is recurrent in nature, like the respiratory flow signal, the analysis is often based on samples extracted from the same segment location of different periods of the signal. Once this segmentation is performed, the entire ensemble is represented by an $L \times N$ data matrix $\mathbf{X}$, where each column $\mathbf{x}_i$ contains L samples of each respiratory cycle and N is the number of successive respiratory cycles:

$$\mathbf{X} = \begin{bmatrix} \mathbf{x}_1 & \mathbf{x}_2 & \cdots & \mathbf{x}_N \end{bmatrix}. \quad (1)$$

Principal component analysis assumes that a signal $\mathbf{x}$ is a zero-mean random process which is characterized by the correlation matrix $\mathbf{R}_x = E[\mathbf{x}\mathbf{x}^{\mathbf{T}}]$. The principal components

Manuscript received April 15, 2011. This work was supported in part by Ministerio de Ciencia e Innovación from Spanish Government under grants TEC2007-68076-C02-01 and TEC2010-21703-C03-01.

A. Garde, B.F. Giraldo and R. Jané are with Dept. of ESAII, Escola Universitaria de Enginyeria Tcnica de Barcelona (EUETIB), Universitat Politècnica de Catalunya (UPC), Institut de Bioenginyeria de Catalunya (IBEC) and CIBER de Bioingeniería, Biomateriales y Nanomedicina (CIBER-BBN). c/. Pau Gargallo, 5, 08028, Barcelona, Spain. (fax: +34 93 401 7045) (e-mail: ainara.garde@upc.edu, beatriz.giraldo@upc.edu, raimon.jane@upc.edu).

L. Sörnmo is with the Department of Electrical and Information Technology and Center of Integrative Electrocardiology, Lund University, Lund SE-221 00, Sweden (e-mail: leif.sornmo@eit.lth.se).

$\mathbf{w}$ result from applying an orthonormal linear transformation $\psi = \begin{bmatrix}\psi_1 & \cdots & \psi_L\end{bmatrix}$ to $\mathbf{x}$ [3],

$$\mathbf{w} = \psi^{\mathbf{T}}\mathbf{x} \tag{2}$$

such that the principal components become mutually uncorrelated.

The orthogonal basis functions are obtained as the most significant eigenvectors of the correlation matrix $\mathbf{R}_x$. In this study, the sample correlation matrix is used, i.e.,

$$\hat{\mathbf{R}}_x = \frac{1}{N}\mathbf{X}\mathbf{X}^{\mathbf{T}}, \tag{3}$$

and thus results from the detected respiratory flow cycles contained in $\mathbf{X}$. Once the eigenvectors and eigenvalues of $\hat{\mathbf{R}}_x$ are calculated, the index R_K is determined which reflects how well the subset of K principal components approximates the ensemble in energy terms,

$$R_K = \frac{\sum_{k=1}^{K}\lambda_k}{\sum_{k=1}^{L}\lambda_k} \tag{4}$$

where K is the number of components.

B. Respiratory flow cycle characterization

Through a moving window applied to the decimated respiratory flow signal ($F_s = 10\ Hz$), a respiratory cycle model is calculated for each window. Since the PB patterns are characterized by cycle lengths between 25 and 100 s (i.e., 0.01-0.04 Hz), a moving window of 30 s, with an overlap of 80%, is selected. The respiratory cycles within the window are detected and aligned to the maximum inspiratory flow placed in the 2nd second, using a fixed cycle duration. The ensemble of respiratory flow cycles within the window, is used to compute the sample autocorrelation matrix $\mathbf{R}_x$. In each window, a respiratory cycle model is obtained as an ensample average of the respiratory cycles using the truncated series expansion as a linear combination of the K eigenvectors weighted by the corresponding principal components. The value of K was determined by requiring that at least 95% of the total energy should be accounted for, and was found to range from 3 to 6.

In order to characterize the morphology of the respiratory flow cycles, a number of parameters are extracted from each cycle model: inspiratory time (Ti), expiratory time (Te), inspiratory flow area (Ai), expiratory flow area (Ae), maximum inspiratory flow value (Mi), maximum expiratory flow value (Me), inspiratory flow kurtosis (Ki), expiratory flow kurtosis (Ke), maximal inspiratory flow instant (Ii), maximal expiratory flow instant (Ie), slope between the inspiration and expiration (Slp), and model error $(Merr)$. The model error is obtained by averaging the mean square error (MSE) between the respiratory cycle model and each of the cycles within the window. Figure 1 illustrates the extraction of the respiratory cycle model and Fig. 2 the related parameters.

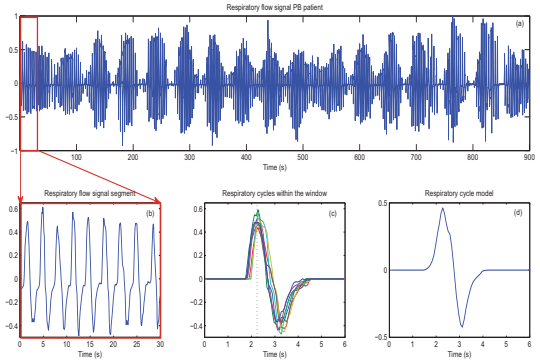

Fig. 1. (a) The respiratory flow signal of a CHF patient with periodic breathing pattern, (b) the respiratory flow signal segment for the selected window, (c) the ensemble of successive cycles within the window, and (d) the respiratory cycle model.

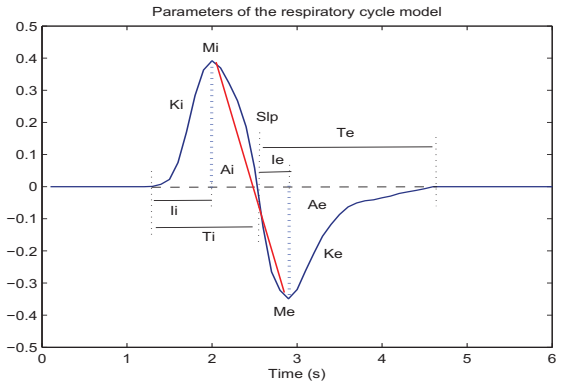

Fig. 2. Parameters extracted from the respiratory cycle model.

III. Datasets

A. Respiratory Data

Respiratory flow signals were recorded from 35 healthy volunteers (12 males, 23 females, aged 26.6±7 years) and 26 patients with CHF (19 males, 7 females, aged 65±9 years) at the Santa Creu i Sant Pau Hospital in Barcelona, Spain. All subjects were studied according to a protocol previously approved by the local ethics committee. The respiratory flow signal was acquired using a pneumotachograph, consisting of a Datex–Ohmeda monitor with a Validyne Model MP45-1-871 Variable-Reluctance Transducer. The signals were recorded at 250 Hz sampling rate.

According to clinical criteria, CHF patients were classified into two groups: 8 patients with periodic breathing pattern and 18 patients with non-periodic breathing pattern.

IV. Results

A. Illustration of the method

Figures 3, 4 and 5 illustrate the performance of PCA when applied to a CHF patient with PB, a CHF patient with nPB, and a healthy subject. From Fig. 3, it is clear that the periodicity is also reflected in the temporal evolution of certain parameters such as inspiratory (Ai) and expiratory (Ae) flow area, expiratory time (Te), maximal inspiratory flow instant (Ii), slope between inspiration and expiration

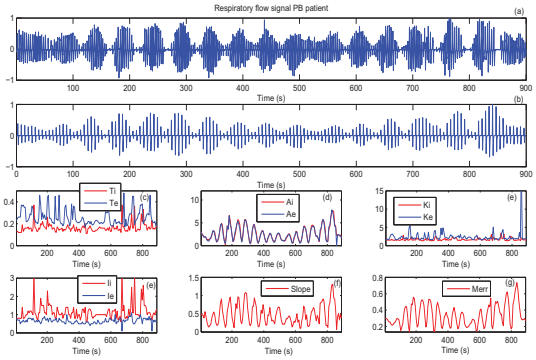

Fig. 3. (a) The respiratory flow signal of a CHF patient with periodic breathing pattern, (b) a new signal created with each cycle model obtained for each window through PCA, (c) inspiratory and expiratory time, (d) inspiratory and expiratory area for each cycle model, (e) inspiratory and expiratory kurtosis, (f) maximal inspiratory and expiratory instant, (g) slope of the respiratory model, and (h) model error for each cycle model.

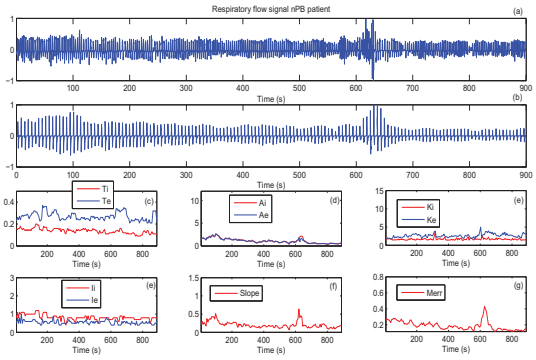

Fig. 4. (a) The respiratory flow signal of a CHF patient with non-periodic breathing pattern, (b) a new signal created with each cycle model obtained for each window through PCA, (c) inspiratory and expiratory time, (d) inspiratory and expiratory area for each cycle model (e) inspiratory and expiratory kurtosis (f) maximal inspiratory and expiratory instant, (g) slope of the respiratory model, and (h) model error for each cycle model.

(Slp), and model error $(Merr)$. No clear periodicity is obvious in Figs. 4 and 5 in (b, d, f and g).

B. Performance Evaluation

The characterization of respiratory flow cycles is evaluated in terms of the following three classification problems: CHF patients with either PB or nPB, CHF patients versus healthy subjects, and nPB patients versus healthy subjects.

Table I presents the mean, standard deviation, and p-value of the most relevant parameters for CHF patients with PB and nPB. The standard deviation of the maximum inspiratory (Mi) and expiratory (Me) flow value are higher in PB patients due to the periodicity. Both Ti and Te are reduced in PB patients.

Table II presents the mean, standard deviation, and p-value of the most relevant parameters for CHF patients and healthy subjects. From Table II it is clear that the maximal expiratory flow instant (Ie) occurs earlier in CHF patients than in healthy subjects. CHF patients exhibit a higher slope. The standard deviation of the expiration time exhibits a lower dispersion in CHF patients than in healthy subjects.

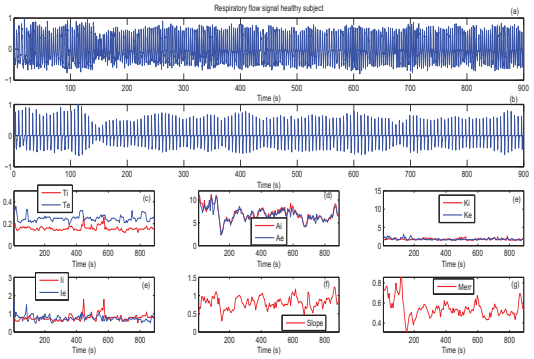

Fig. 5. (a) The respiratory flow signal of a healthy subject, (b) a signal created with each cycle model obtained for each window through PCA, (c) inspiratory and expiratory time, (d) inspiratory and expiratory area for each cycle model, (e) inspiratory and expiratory kurtosis, (f) maximal inspiratory and expiratory instant (g) slope of the respiratory model, and (h) model error for each cycle model.

Table III presents the mean, standard deviation, and p-value of the most relevant parameters for nPB patients and healthy subjects. Like in CHF patients, the maximal expiratory flow instant (Ie) occurs earlier in nPB patients than in healthy subjects, with a higher slope. The standard deviation of the expiratory time is lower in nPB patients than in healthy subjects.

TABLE I
CHF PB VS. NPB $\mu \pm \sigma$

	PB	**nPB**	p-**value**
$M-Merr$	0.37 ± 0.12	0.27 ± 0.12	0.02
$M-Ti$	1.16 ± 0.27	1.38 ± 0.23	0.05
$M-Te$	1.79 ± 0.34	2.21 ± 0.31	0.02
$M-Mi$	0.44 ± 0.05	0.36 ± 0.11	0.05
$M-Me$	0.34 ± 0.07	0.26 ± 0.10	0.03
$M-Slp$	0.66 ± 0.20	$0,45 \pm 0.20$	0.03
$SD-Merr$	0.19 ± 0.09	0.11 ± 0.05	0.04
$SD-Te$	0.22 ± 0.05	0.34 ± 0.15	0.03
$SD-Ai$	0.86 ± 0.40	0.49 ± 0.19	0.04
$SD-Ae$	0.84 ± 0.40	0.49 ± 0.19	0.05
$SD-Mi$	0.13 ± 0.05	0.07 ± 0.03	0.005
$SD-Me$	0.10 ± 0.04	0.05 ± 0.02	0.003
$SD-Slp$	0.27 ± 0.11	0.17 ± 0.09	0.04

TABLE II
CHF VS. HEALTHY $\mu \pm \sigma$

	CHF-pat	**HEALTHY**	p-**value**
$M-Merr$	0.30 ± 0.13	0.25 ± 0.16	0.02
$M-Ti$	1.31 ± 0.26	1.63 ± 0.39	< 0.0005
$M-Te$	2.08 ± 0.37	2.72 ± 0.75	< 0.0005
$M-Ki$	1.72 ± 0.10	1.81 ± 0.15	0.009
$M-Mi$	0.39 ± 0.10	0.32 ± 0.13	0.02
$M-Me$	0.28 ± 0.10	0.18 ± 0.09	< 0.0005
$M-Ie$	0.63 ± 0.15	0.97 ± 0.35	< 0.0005
$M-Slp$	0.51 ± 0.22	0.24 ± 0.15	< 0.0005
$SD-Ti$	0.19 ± 0.07	0.31 ± 0.14	< 0.0005
$SD-Te$	0.30 ± 0.14	0.66 ± 0.40	< 0.0005
$SD-Ki$	0.18 ± 0.07	0.33 ± 0.18	< 0.0005
$SD-Ke$	0.49 ± 0.31	0.68 ± 0.51	0.03
$SD-Mi$	0.09 ± 0.04	0.06 ± 0.02	0.01
$SD-Me$	0.07 ± 0.03	0.04 ± 0.02	0.003
$SD-Ii$	0.18 ± 0.08	0.28 ± 0.11	< 0.0005
$SD-Ie$	0.13 ± 0.07	0.29 ± 0.20	< 0.0005
$SD-Slp$	0.20 ± 0.10	0.11 ± 0.05	< 0.0005

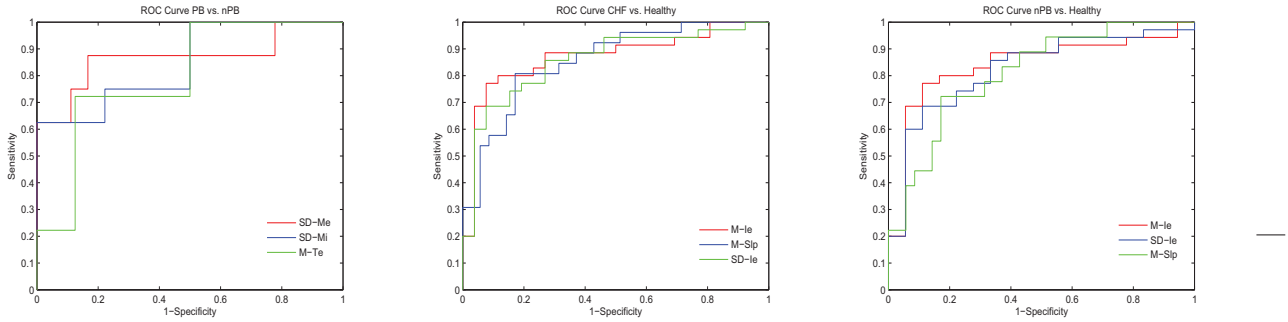

(a) AUC
$SD-Me$: 87%
$SD-Mi$: 85%
$M-Te$: 80%

(b) AUC
$M-Ie$: 87%
$SD-Ie$: 86%
$M-Slp$: 86 %

(c) AUC
$M-Ie$: 84%
$SD-Ie$: 82%
$M-Slp$: 81 %

Fig. 6. ROC curves obtained with (a) $SD-Me$, $SD-Mi$, $M-Te$, classifying PB versus nPB patients, (b) $M-Ie$, $SD-Ie$, $M-Slp$, classifying CHF patients versus healthy subjects, and (c) $M-Ie$, $SD-Ie$, $M-Slp$, classifying nPB patients versus healthy subjects.

TABLE III
NPB VS. HEALTHY $\mu \pm \sigma$

	nPB-pat	**HEALTHY**	***p*-value**
$M-Ti$	1.38 ± 0.23	1.63 ± 0.40	0.005
$M-Te$	2.21 ± 0.31	2.72 ± 0.75	0.009
$M-Ki$	1.72 ± 0.08	1.81 ± 0.15	0.03
$M-Me$	0.26 ± 0.10	0.18 ± 0.09	0.01
$M-Ie$	0.66 ± 0.16	0.97 ± 0.35	< 0.0005
$M-Slp$	0.45 ± 0.20	0.24 ± 0.15	< 0.0005
$SD-Ti$	0.20 ± 0.07	0.31 ± 0.14	0.001
$SD-Te$	0.34 ± 0.15	0.66 ± 0.40	0.001
$SD-Ki$	0.17 ± 0.08	0.33 ± 0.18	< 0.0005
$SD-Ii$	0.19 ± 0.09	0.28 ± 0.11	0.006
$SD-Ie$	0.14 ± 0.08	0.29 ± 0.20	< 0.0005
$SD-Slp$	0.17 ± 0.09	0.11 ± 0.05	0.004

Figures 6(a) – (c), correspond to the classification of PB versus nPB into CHF patients, CHF patients versus healthy subjects, and nPB patients versus healthy subjects, respectively, with the three most statistically significant parameters. The best result classifying PB and nPB patients is obtained with the standard deviation of the maximum expiratory flow value, with an accuracy of 87%. When classifying CHF patients and healthy subjects, the best result is obtained with the mean of the maximal expiratory flow instant, with an accuracy of 87%. Finally, the best result classifying nPB patients and healthy subjects is achieved with the mean of the maximal expiratory flow instant, with an accuracy of 84%.

V. CONCLUSIONS

When classifying PB patients and nPB patients, the standard deviation of the maximum inspiratory flow value and foremost the standard deviation of the maximum expiratory flow value are much higher in PB patients, which could be related to the periodicity these patients (accuracy of 87%). Both inspiratory and expiratory times are reduced in PB patients.

The maximal expiratory flow instant occurs before and with lower dispersion in CHF patients than in healthy subjects (accuracy of 87%). CHF patients present a higher slope between inspiration and expiration with lower inspiratory and expiratory times than in healthy subjects.

When comparing nPB patients versus healthy subjects, the maximal expiratory flow occurs earlier and with a lower dispersion in nPB patients than in healthy subjects (accuracy of 84%). Likewise, nPB patients present reduced inspiratory and expiratory time and higher slope than in healthy subjects.

In addition to the differences found previously in the respiratory pattern CHF patients and healthy subjects [7], [8] present significant differences in their respiratory flow cycle. As a preliminary study, these results suggest that the analysis of the respiratory cycle morphology is a promising approach to evaluate differences between CHF patients and healthy subjects.

VI. ACKNOWLEDGMENTS

The authors would like to thank to Drs. S. Benito and A. Bayés-Genis and their collaborators of Santa Creu i Sant Pau Hospital, Barcelona, Spain, for their collaboration in the signal database acquisition.

REFERENCES

[1] I. T. Joliffe, *Principal Component Analysis*. Springer, New York, NY, USA, 2002.

[2] D. Hamilton, J. McQueen, and W. Sandham, "Improved pca-based electrocardiogram data compression using variable-length asymmetric beat vectors," *EURASIP Journal on Applied Signal Processing*, vol. 6, no. 4, pp. 194–202, 1999.

[3] F. Castells, P. Laguna, L. Sörnmo, A. Bollmann, and J. Millet, "Principal component analysis in ecg signal processing," *EURASIP Journal on Advances in Signal Processing*, 2007.

[4] L. AlDabal and A. BaHammam, "Cheyne-stokes respiration in patients with heart failure," *Lung*, vol. 188, pp. 5–14, 2010.

[5] P. A. Lanfranchi, A. Braghiroli, E. Bosimini, G. Mazzuero, R. Colombo, C. F. Donner, and P. Giannuzzi, "Prognostic value of nocturnal Cheyne–Stokes respiration in chronic heart failure," *Circulation*, vol. 99, no. 11, pp. 1435–1440, 1999.

[6] G. D. Pinna, R. Maestri, A. Mortara, P. Johnson, T. Witkowski, P. Ponikowski, D. Andrews, S. Capomolla, M. La Rovere, and P. Sleight, "Nocturnal periodic breathing is an independent predictor of cardiac death and multiple hospital admissions in heart failure," in *Proc. Comput. Cardiol.* IEEE Press, 2006, pp. 837–840.

[7] A. Garde, L. Sörnmo, R. Jané, and B. Giraldo, "Breathing pattern characterization in chronic heart failure patients using respiratory flow signal," *Ann. Biomed. Eng.*, vol. 38, no. 12, pp. 3572–3580, 2010.

[8] ——, "Correntropy-based spectral characterization of respiratory patterns in patients with chronic heart failure," *IEEE Trans. Biomed. Eng.*, vol. 57, no. 8, pp. 1964–1972, 2010.